High-intensity focused ultrasound-induced mechanochemical transduction in synthetic elastomers

Gun Kim[a,b], Vivian M. Lau[a,c], Abigail J. Halmes[a,c], Michael L. Oelze[a,b,d], Jeffrey S. Moore[a,b,c,e,1], and King C. Li[a,b,f,1]

[a]Beckman Institute for Advanced Science and Technology, University of Illinois at Urbana–Champaign, Urbana, IL 61801; [b]Carle Illinois College of Medicine, University of Illinois at Urbana, Urbana–Champaign, Urbana, IL 61820; [c]Department of Chemistry, University of Illinois at Urbana–Champaign, Urbana, IL 61801; [d]Department of Electrical and Computer Engineering, University of Illinois at Urbana–Champaign, Urbana, IL 61801; [e]Department of Materials Science and Engineering, University of Illinois at Urbana–Champaign, Urbana, IL 61801; and [f]Department of Bioengineering, University of Illinois at Urbana–Champaign, Urbana, IL 61801

While study in the field of polymer mechanochemistry has yielded mechanophores that perform various chemical reactions in response to mechanical stimuli, there is not yet a triggering method compatible with biological systems. Applications such as using mechanoluminescence to generate localized photon flux in vivo for optogenetics would greatly benefit from such an approach. Here we introduce a method of triggering mechanophores by using high-intensity focused ultrasound (HIFU) as a remote energy source to drive the spatially and temporally resolved mechanical-to-chemical transduction of mechanoresponsive polymers. A HIFU setup capable of controlling the excitation pressure, spatial location, and duration of exposure is employed to activate mechanochemical reactions in a cross-linked elastomeric polymer in a noninvasive fashion. One reaction is the chromogenic isomerization of a naphthopyran mechanophore embedded in a polydimethylsiloxane (PDMS) network. Under HIFU irradiation evidence of the mechanochemical transduction is the observation of a reversible color change as expected for the isomerization. The elastomer exhibits this distinguishable color change at the focal spot, depending on ultrasonic exposure conditions. A second reaction is the demonstration that HIFU irradiation successfully triggers a luminescent dioxetane, resulting in localized generation of visible blue light at the focal spot. In contrast to conventional stimuli such as UV light, heat, and uniaxial compression/tension testing, HIFU irradiation provides spatiotemporal control of the mechanochemical activation through targeted but noninvasive ultrasonic energy deposition. Targeted, remote light generation is potentially useful in biomedical applications such as optogenetics where a light source is used to trigger a cellular response.

high-intensity focused ultrasound | mechanochromism | mechanophores | mechanoluminescence | spatiotemporal control

Mechanical force exerted on a covalent bond acts as an energetic stimulus to drive specific chemical reactivity (mechanochemistry) (1). Particularly, mechanophores, i.e., mechanically sensitive molecules, have attracted attention due to their role in eliciting various chemical transformations in polymers (2). Extensive work in molecular design has revealed a rich library of mechanophores, which when subjected to mechanical stress undergo selective bond cleavage to unveil color change (3, 4), fluorescence (5), new reactive functionality (6), catalytic activity (7), light emission (8), and small-molecule release (9), among other responses. The ability of mechanochromic mechanophores to "visualize" the mechanical response to applied force provides insight for identifying the damage location and the material state in polymeric materials. Of particular importance to extending functionality of these mechanophores is the development of novel force-control tools capable of noninvasively triggering their activation. Mechanochemical responses have been observed when mechanical energy is applied to bulk-phase materials via mechanisms such as compression (10, 11), tension (3, 4), and shock wave (12, 13), or to solution-phase polymers and polymer interfaces via ultrasonic cavitation (3, 14, 15). The ability to access a wide range of chemical reactivity via mechanical force has led researchers to consider the applicability of polymer mechanochemistry in biomedical applications as a platform for drug delivery (16–19) or sensing and self-reporting materials (20–22). To uncover the potential of polymer mechanochemistry in biological regimes, it is necessary to have a stimulus that provides on-demand, spatiotemporally resolved mechanical energy in a noninvasive and biocompatible manner.

Recently, high-intensity focused ultrasound (HIFU) has gained attention as a remote energy source for therapeutic intervention due to its noninvasive nature and superior ability to penetrate biological tissues compared with other spatiotemporally resolved stimuli such as light. By focusing an ultrasonic wave onto the target location, the high intensity of irradiation affects mechanical deformation and cavitation in response to the acoustic pressure wave, as well as localized heating from energy dissipation. HIFU has demonstrated clinical success in applications including tumor ablation (23, 24), pain management (25), neurosurgery (26–29),

Significance

One challenge in exploiting polymer mechanochemistry in biological and clinical regimes is the lack of a compatible triggering system that enables noninvasive, spatiotemporal control of mechanochemical transformations. Here we address this problem through an approach that uses high-intensity focused ultrasound (HIFU), controlling the spatial location and period of mechanophore activation without causing irreversible damage to the sample. As a proof of concept, we provide the demonstration of the capability of a HIFU-based triggering system to activate two different mechanochemical responses: a reversible color change, and the emission of light. The results highlight the HIFU system as a stimulus that provides on-demand, spatiotemporally resolved mechanical energy, and makes polymer mechanochemical transduction a potential means for minimizing invasive biomedical methods.

and drug delivery (16, 30). Indeed, polymer-based drug-delivery platforms that rely on heat-induced release mechanisms are triggered by long-duration, pulsed HIFU irradiation (31–33). Nonetheless, the use of HIFU to trigger polymer mechanochemistry has thus far only been demonstrated in micellar systems (34).

In this work, we evaluate the ability of HIFU to trigger polymer mechanochemistry in a polydimethylsiloxane (PDMS) elastomeric network through mechanical deformation. Our group has previously reported naphthopyran (NP) as a colorless mechanophore that undergoes electrocyclic ring opening, generating an orange-colored merocyanine in response to mechanical force (4). The visible color change associated with NP mechanoactivation provides a simple readout for initial investigations of the HIFU-triggered polymer mechanochemistry. By irradiating NP–cross-linked PDMS elastomer samples with HIFU, we show that short sonication durations at moderate power and output pressures provide the optimal conditions to achieve mechanically induced mechanophore activation within bulk materials. Further, we demonstrate that the same HIFU conditions successfully activate a mechanoluminescent mechanophore to emit blue light. Finally, based on the features we observed, directions for therapeutic applications of the mechanophores are discussed.

Results

Design of Mechanoactive Polymer and HIFU-Based Triggering System.

At the outset of our studies, cross-linked PDMS elastomer emerged as the ideal bulk matrix to investigate HIFU-triggered polymer mechanochemistry due to the biocompatibility of the material as well as the ease of covalent functionalization via hydrosilylation to incorporate mechanophores. NP-incorporated cross-linked elastomeric PDMS specimens were prepared as 1.5- and 5-mm-thick films according to Robb et al. (4), using bisvinyl-terminated, mechanoactive NP (Fig. 1*A*) (35) or the monovinyl NP control, which is mechanically inactive and serves as a control (Fig. 1*B*). The hydrosilylation reaction covalently incorporates these NPs into the elastomer by cross-linking the PDMS matrix at the position of the vinyl handles. The molecular positions of the bisvinyl attachment points in the NP mechanophore effectively transmit mechanical force to the mechanophore's C–O pyran bond to drive electrocyclic ring opening. On the other hand, the NP control containing a single vinyl terminus does not experience significant molecular deformation when mechanical force is applied to the PDMS network (Fig. 1*B*). Consistent with previous results (4), 1.5-mm-thick PDMS films functionalized with 1.5 wt % of NP (NP-PDMS) show color change under mechanical force, exerted by compression with a blunt-tipped stylus (*SI Appendix, SI Materials and Methods* and Fig. S1). This color change is reversible under ambient conditions within 10 min. In contrast, the same mechanical stimulus does not result in observable color change with an identically prepared sample for which the NP control is used in place of NP. Films of PDMS covalently functionalized with either NP or NP-control exhibit color change when irradiated with 365-nm UV light or when heated to 100 °C, demonstrating photo- and thermochromism (*SI Appendix,* Fig. S1).

The proposed HIFU-based triggering system is illustrated in Fig. 2*A*. Spatial control of mechanoactive response was achieved by using a computer-controlled micropositioning stage capable of locating the sample-holder assembly with 2-µm spatial accuracy (*Materials and Methods* and *SI Appendix,* Fig. S2*B*). The irradiation of solid polymers with HIFU is known to result in local heating at the interior of the bulk material, which accumulates thermal energy upon prolonged sonication (36). We therefore examined the interaction of HIFU with PDMS to determine the extent of thermal effects on the samples and thus the temporal resolution. A 1.5-mm-thick film of unfunctionalized PDMS (i.e., without any NP functionalization) was first irradiated with continuous-wave (CW) ultrasound at a frequency of 1

MHz for 5 to 7 s, and the spatial-peak temporal average intensity (I_{SPTA}) of the beam varied from 39.4 to 376 W·cm^{-2} (peak acoustic pressure amplitude, 1.1–3.4 MPa) (*SI Appendix, SI Materials and Methods*). At intensities less than or equal to 354 W·cm^{-2} (3.3 MPa), no change in the material was visually observed in the unfunctionalized PDMS film. However, upon irradiation at 376 W·cm^{-2} (3.4 MPa), irreversible opacification of the film at the focal spot was observed (Fig. 2 *B, b2*). In addition, the formation of small bubbles was observed near the focal spot, providing additional evidence of thermal ablation (Fig. 2 *B, b2*). Similarly, when the NP-PDMS films were irradiated with CW-HIFU at intensities exceeding ~354 W·cm^{-2}, ablation of the material was observed, resulting in irreversible discoloration (orange) of the film accompanied by bubble formation at the focal spot (Fig. 2 *B, b3*). Both observations indicate that a lower intensity (<376 W·cm^{-2}) is desirable to avoid thermal effects that mask the mechanochromic changes. During ultrasonic irradiation, a thermocouple was used to track the temperature increase in the focal region. Only minor increases in temperature (<6 °C) were observed at intensities below 354 W·cm^{-2} (3.3 MPa) for 7 s (Fig. 2 *C, c1*). However, the intensity–temperature relationship indicated that the temperature development around the focal spot would be significant from 354 W·cm^{-2} upward, suggesting that thermal ablation would be more dominant than mechanical activation as evident from the irreversible material damage observed (*Materials and Methods*).

To further rule out thermal activation, a 1.5-mm-thick PDMS film functionalized with the NP control was exposed to the same CW-HIFU conditions. The NP control (Fig. 1*B*) is photo- and thermally activated but does not exhibit color change in response to mechanical deformation. When sonicating NP control, no visible color change was observed at $I_{SPTA} \leq 333$ W·cm^{-2} (3.2 MPa) (Movie S1). The absence of color change in the NP-control PDMS suggests that the HIFU sonication does not provide sufficient thermal energy to cause NP isomerization at intensities less than or equal to 333 W·cm^{-2}. However, when the film was irradiated with intensities greater than 376 W·cm^{-2} (>3.4 MPa), the focal spot promptly exhibited irreversible material damage and color change due to the thermal threshold being reached (Fig. 2 *B, b4*). Therefore, using our HIFU setup, significant thermal effects can occur at $I_{SPTA} \geq 376$ W·cm^{-2}, which triggers thermochromism in NP and also results in irreversible material damage of the PDMS.

Mechanical Activation of NP Using HIFU.

Having determined the threshold intensity (≤ 333 W·cm^{-2}) and sonication duration (7 s) to minimize the thermal effects of CW-HIFU irradiation on PDMS, we evaluated the ability of HIFU to induce a color change in NP-PDMS via mechanical force, i.e., acoustic radiation force (*SI Appendix, SI Materials and Methods*). Radiation force occurs because ultrasonic energy is absorbed by the medium (37). This results in a transfer of momentum from the wave to the medium resulting in a radiation force in the direction of wave propagation. The radiation force is proportional to the time-average intensity of the wave times the absorption coefficient of the medium (see equation 10 of ref. 37). Using a 1-MHz transducer, a 1.5-mm-thick NP-PDMS film was irradiated with CW-HIFU for 7 s at 3.2 MPa ($I_{SPTA} = 333$ W·cm^{-2}). A color change from colorless to orange was visually observed at the focal spot, demonstrating localized mechanophore activation triggered by HIFU irradiation (Fig. 2 *C, c2–c4* and Movie S2). After sonication, the orange color dissipated under ambient light and temperature within 1 min. The color change during HIFU sonication was qualitatively characterized by red-green-blue (RGB) analysis (*SI Appendix, SI Materials and Methods* and Fig. S3). Formation of the orange merocyanine (red = 236; green = 227; and blue = 174) from the colorless NP (red = 238; green = 234; and blue = 226) was characterized by a consistent
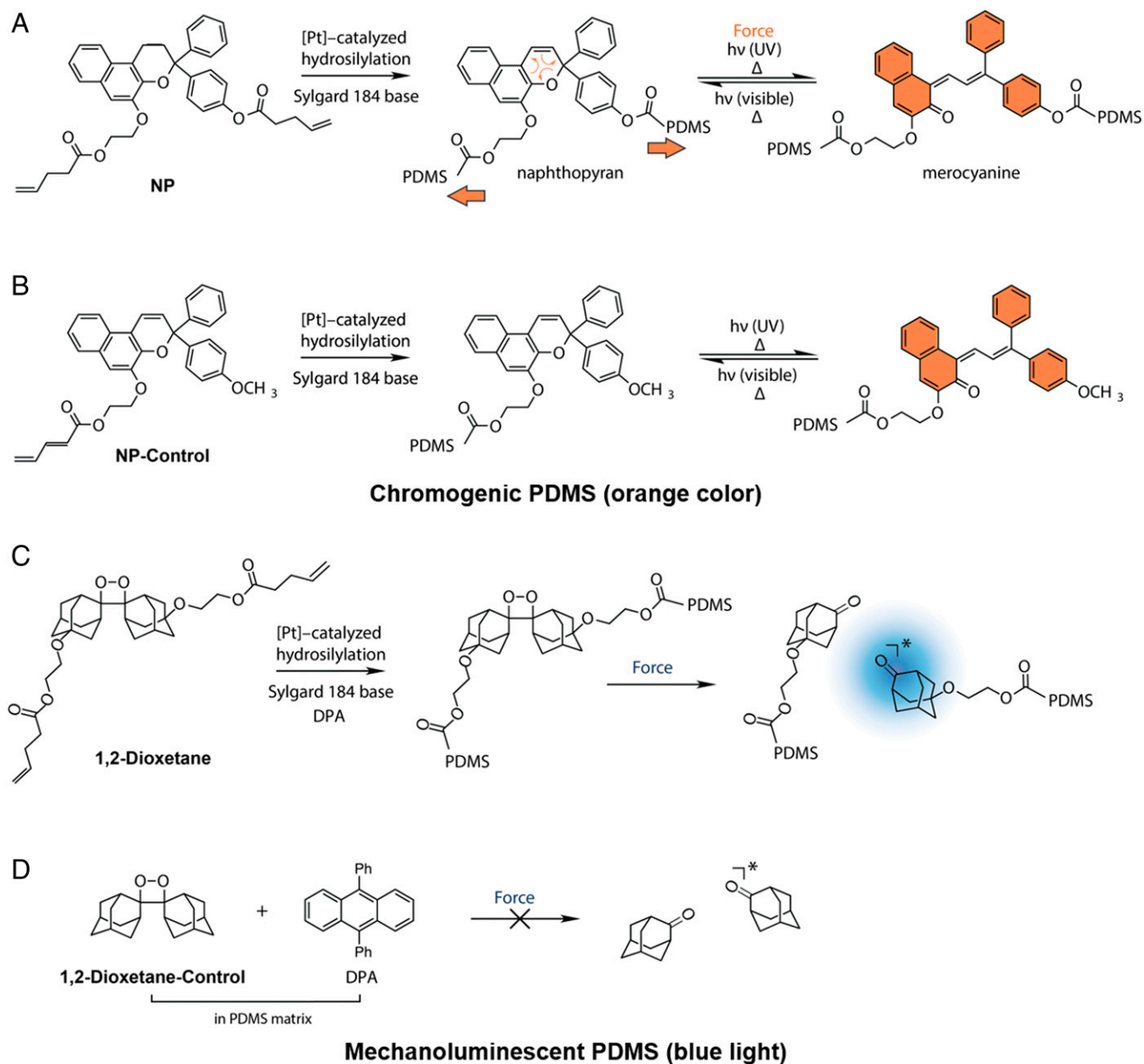
Fig. 1. Synthesis of mechanochromic and mechanoluminescent PDMS materials: (*A*) NP (bisvinyl-terminated naphthopyran, 1.5 wt %) is cross-linked into the PDMS network and isomerizes in response to mechanical force to generate an orange-colored merocyanine species; (*B*) Monofunctional NP control (1.5 wt %) is covalently appended to PDMS and insensitive to mechanical force. Both NP and NP-control isomerize to the colored merocyanine form under UV light and high temperature; (*C*) Dioxetane (1.5 wt %) is cross-linked into the PDMS network and undergoes a cycloelimination reaction in response to mechanical force to generate blue light in the presence of 0.5 wt % of the sensitizer DPA; and (*D*) Physically incorporating 1.5 wt % dioxetane control with 0.5 wt % DPA gives an elastomeric control material that is insensitive to mechanical force.

and significant shift in the blue channel (Fig. 3*B* and *SI Appendix*, Fig. S3*B*). Six seconds after HIFU irradiation ceased, the RGB profile returned to values (red = 243; green = 236; and blue = 221) nearly identical to the original sample. These observations are consistent with HIFU-triggered isomerization of NP to highly colored merocyanine, followed by reversion to colorless NP under ambient light after cessation of the HIFU irradiation. Indeed, when the identical focal spot on the NP-PDMS sample was repeatedly sonicated with HIFU, the same colorless-to-orange transition of NP was observed every time followed by color reversion, demonstrating that the mechanochromic behavior was reversible and repeatable and the specific ultrasonic conditions did not cause noticeable chemical damage to NP. Unlike CW-

HIFU irradiation, tone-burst excitation, even with a duty cycle of 90%, which corresponds to an I_{SPTA} of 300 W·cm^{-2} and a 10% decrease in the radiation force, did not result in visually observable mechanochromism, showing that mechanical force generated with tone-burst excitation was not sufficient to activate the NP-PDMS films with a 7-s sonication duration.

At the HIFU intensity used (I_{SPTA} = 333 W·cm^{-2}) the contribution of thermal energy to the observed mechanochromism in NP-PDMS is likely negligible. Because a PDMS film of identical dimensions functionalized with the NP control did not exhibit observable color change when irradiated at this intensity (Movie S1), the primary effect of HIFU in this intensity regime is the transfer of mechanical energy to the PDMS film. The
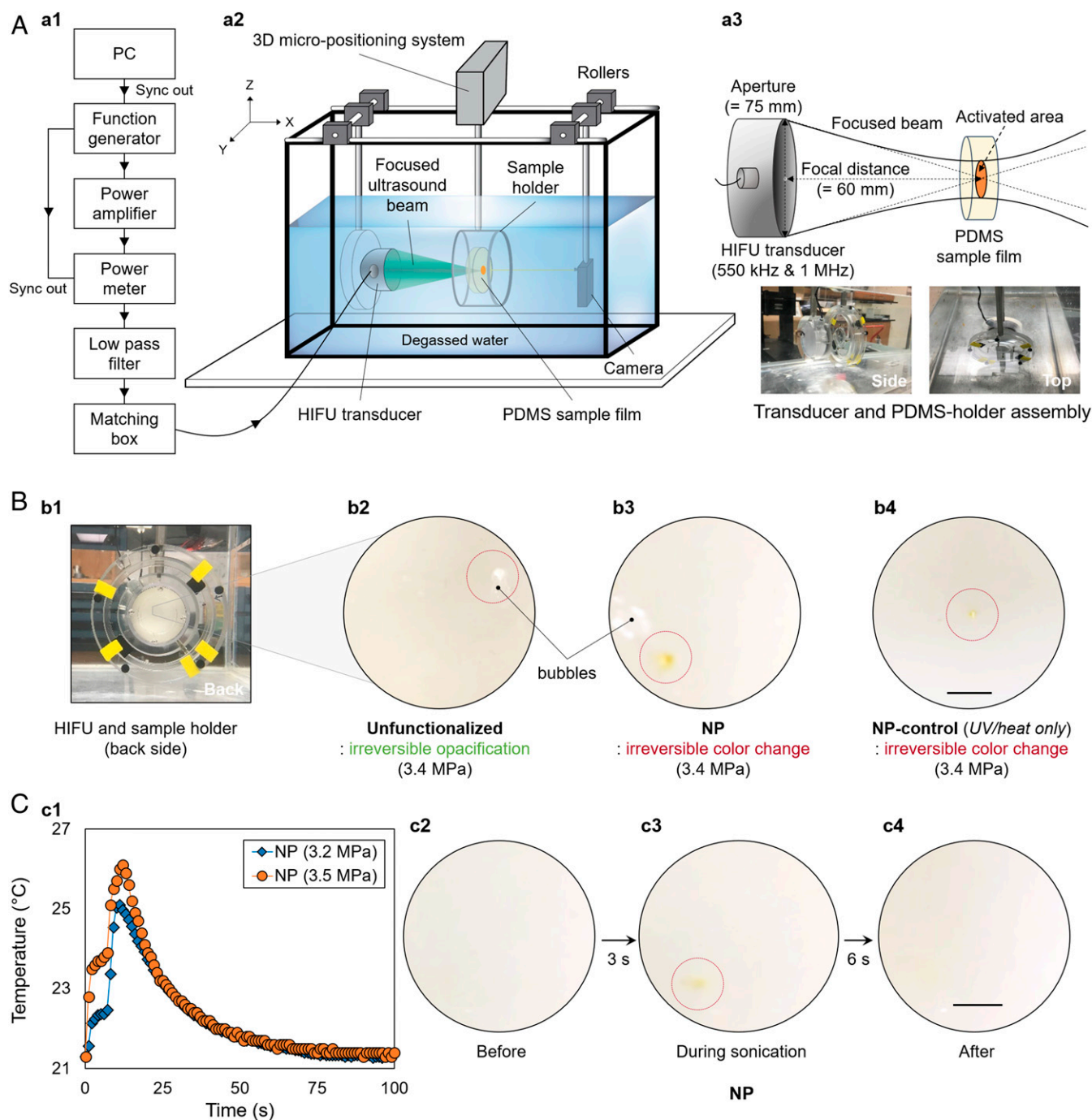
Fig. 2. HIFU-induced mechanochromic response of the NP-PDMS elastomer under 1-MHz CW (sonication time of 7 s): (*A*) schematic of the experimental setup and characteristics of the HIFU transducer (*SI Appendix, SI Materials and Methods*); (*B*) irreversible material damage with thermal ablation (unfunctionalized PDMS and NP) and example of thermally induced activation at 3.4 MPa (NP control); and (*C*) temperature (averaged) increase during the HIFU irradiation (3.2 vs. 3.5 MPa) and observed reversible color change in the NP-PDMS elastomer. Only mild temperature increases (~4 °C) occur at the focal spot during sonication. (Scale bar: 2.5 mm.)

observation of chromogenicity in NP-PDMS is therefore attributed to HIFU-induced triggering of the cross-linked NP mechanophore. Exposing 1.5-mm-thick NP-PDMS films to 7 s of CW-HIFU irradiation at pressure levels from 2.3 to 3.2 MPa resulted in visibly evident reversible color change (colorless to orange) while the brightness of the orange color corresponded to the applied pressure. Below 2.3 MPa of acoustic pressure (I_{SPTA} < 172 W·cm^{-2}), no distinguishable color change was observed at the focal spot, indicating that at lower intensities,

mechanical force applied to the PDMS sample is insufficient to activate the NP mechanophore. At all pressure levels where mechanophore activation was observed, the diameter of the activated colored area was ~1 mm, which is comparable to the estimated beamwidth at the focal spot (*SI Appendix, SI Materials and Methods*). This observation suggests that mechanophore activation is localized to the focal spot and the dimension of the colored area is determined by the beamwidth. Taken together, these results indicate that CW-HIFU applied to NP-PDMS at
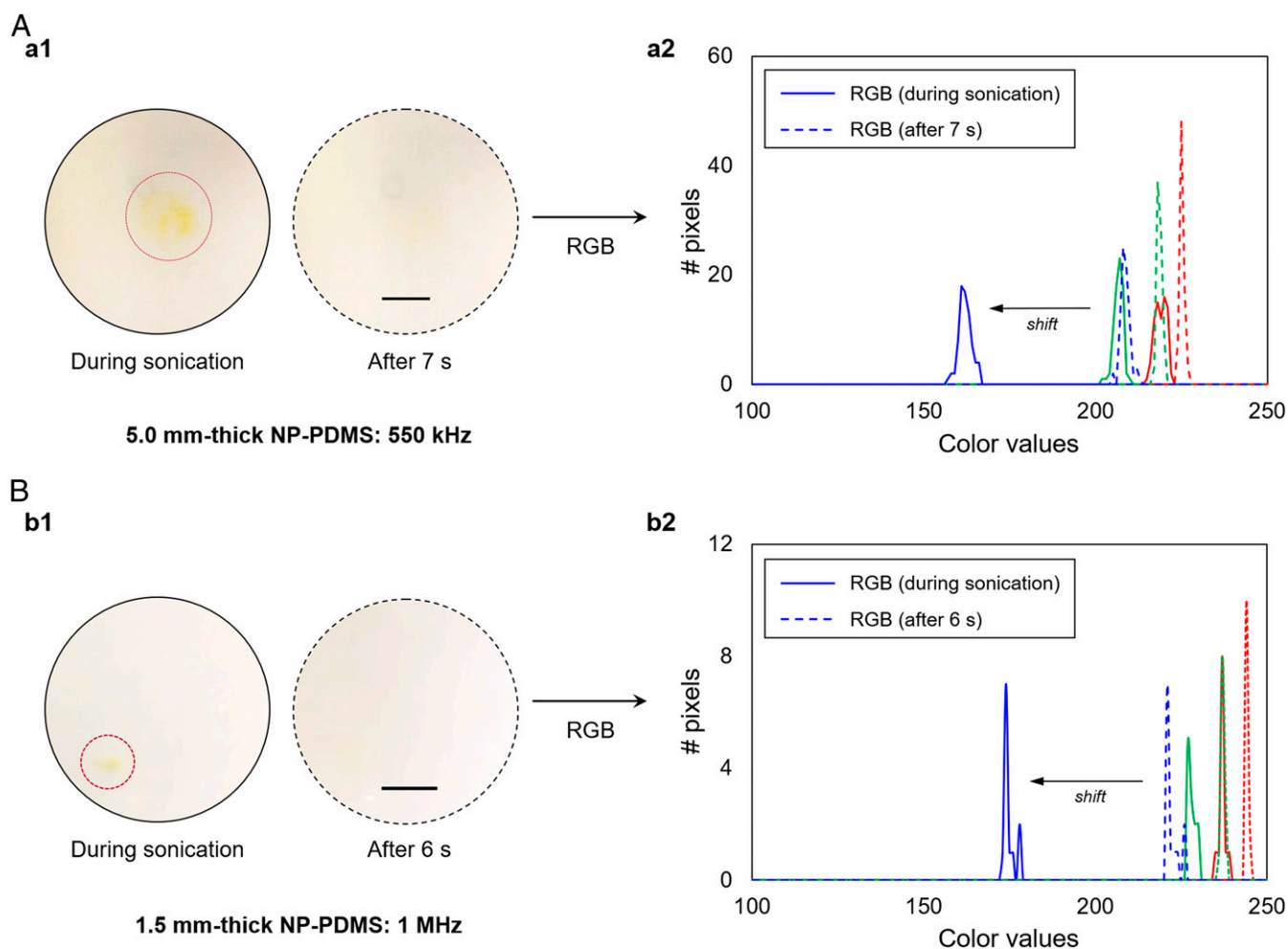
Fig. 3. Dependency of color change on the excitation frequency. Size of activated area correlates to the wavelength and beamwidth of the transducer. (*A*) A 550-kHz HIFU transducer results in the colored area having a diameter of 2.7 mm. (*B*) A 1-MHz HIFU transducer results in the colored area having a diameter of 1.2 mm. The RGB analysis during sonication provides a color profile that is consistent with NP electrocyclic ring opening. (Scale bar: 2.5 mm.)

acoustic pressures between 2.3 and 3.2 MPa triggers color change with spatial and temporal resolution corresponding to the focal spot of the HIFU source, thus acting as a trigger for polymer mechanochemistry.

Effect of Excitation Frequency: 1 MHz vs. 550 kHz. We next examined the correlation between the mechanochromism of the cross-linked NP and the excitation frequency of the HIFU transducer. A 1-MHz (beamwidth at the focus of 1.2 mm) transducer and a 550-kHz (beamwidth at the focus of 2.2 mm) transducer were used to deliver the same acoustic pressure of 3.2 MPa (I_{SPTA} = 333 W·cm^{-2}) to the target areas of 1.5- and 5.0-mm-thick NP-PDMS films, respectively. Note that the sample thickness was determined based on the depth of field of the transducers (*SI Appendix, SI Materials and Methods*). Similar to the results above (Figs. 2*C* and 3*B*), reversible color changes in the regions of the focal spots were observed for both samples—a visible orange coloration appeared during the sonication period, which disappeared within 1 min after the end of irradiation (Fig. 3*A* and Movie S3). However, for the activated area, the diameter of the orange-colored area obtained from irradiation of the 5.0-mm-thick film with a 550-kHz beam was approximately two times larger than that achieved using a HIFU frequency of 1 MHz (Fig. 3 and *SI Appendix*, Fig. S4). This clearly shows that the size of the activated area was determined by the beamwidth of the

transducer, supporting the ability of the HIFU setup to modulate the size of mechanophore activation over multiple frequencies. After color dissipation following an initial sonication event, irradiation of the same area resulted in a repeated chromogenic response within the selected pressure-level range (2.3–3.2 MPa). The RGB analysis also shows a concomitant shift in the blue channel during the HIFU irradiation, while the red and green channels exhibited no significant changes (Fig. 3 *A*, a*2* and Fig. 3 *B*, b*2*). With a temporal resolution of 7 s, this consistency demonstrates that our HIFU setup is capable of spatially controlling the activation of NP mechanophore in PDMS.

HIFU Sonication Through the Skull: Potential for Biomedical Applications. HIFU is an emerging noninvasive stimulus for drug delivery as it is able to deeply penetrate tissue in comparison with visible and near-infrared light (29). A potential concern for noninvasive in vivo biomedical applications of HIFU is significant wave distortion (e.g., attenuation) arising from interactions with intervening media such as the skull tissue. To demonstrate the viability of using HIFU as a stimulus to trigger polymer mechanochemistry in a biological context, we examined the activation of polymer mechanochemistry through a sample of mouse skull (~300–400-μm thick) that acts as an attenuating and aberrating layer. The skull tissue was attached to the anterior surface of a hemisphere-shaped PDMS slab (15 mm at the

thickest point) (Fig. 4A). Then, a 550-kHz HIFU transducer was used to propagate the ultrasonic beam behind the surface of the PDMS–skull assembly. First, we quantified the energy loss of the ultrasonic beam through the skull using a hydrophone. As shown in the received time-domain signal (Fig. 4B), the presence of the skull tissue reduced the peak intensity amplitude by ∼16%. Thus, a relatively higher excitation voltage was required for visible color change with intervening tissues, compared with the sample without tissue layer. Our experimental results suggest that the estimated activation threshold pressure and the maximum pressure for this boundary condition are 2.5 and 3.4 MPa (I_{SPTA} of 204–376 W·cm^{-2}), respectively. We further verified that above 3.5 MPa (I_{SPTA} = 399 W·cm^{-2}), the hemisphere PDMS underwent irreversible thermal ablation rather than exhibiting mechanical irradiation effects. To examine mechanophore activation at different penetration depths, we varied the location of the focal spot from the surface to the back of the assembly in 0.5-mm increments (in the x direction) and identified that within the hemisphere geometry considered, the acoustic energy achieved the maximum color change in terms of both intensity and diameter of the chromogenic region at ∼5 mm below the PDMS–skull assembly. Matching the HIFU conditions used with NP-PDMS films, we then sonicated the PDMS–skull assembly using an acoustic pressure of 3.2 MPa (I_{SPTA} = 333 W·cm^{-2}) and irradiation time of 7 s at this sample depth. During the sonication period, a distinguishable change to orange color was recorded (Fig. 4 C and D), showing that isomerization of NP was achieved by the HIFU irradiation in the target area. Color dissipation was observed within 1 min after cessation of HIFU irradiation, demonstrating the reversibility of mechanically activated NP isomerization (Fig. 4E and Movie S4). HIFU-based triggering of polymer mechanochemistry through a mouse skull demonstrates the potential for in vitro/in vivo applications (23, 25, 26). With the capability to spatiotemporally control the acoustic pressure, HIFU enables the activation of mechanophore-functionalized biocompatible polymers (3, 38), potentially facilitating mechanochemical phenomena such as mechanoluminescence in vivo through intervening tissues such as bone. In the context of clinical applications, it is important to note that careful control of HIFU energy deposition into tissue is required to prevent undesirable thermal/mechanical damage to surrounding tissue, e.g., coagulative necrosis (28). The Bioeffects Committee of the American Institute of Ultrasound in Medicine has issued important guidelines for the safe use of ultrasound for therapeutic applications (39). Currently, for thermal-based therapeutic applications of HIFU, MRI (MR-guided HIFU) is the standard of care (40) and for nonthermal (i.e., mechanical) therapeutic applications of HIFU, ultrasonic visualization of the HIFU beam can be used to monitor therapy application (41).

Mechanoluminescence by HIFU. As light is an important stimulus in biomedicine, we chose to test the ability of HIFU to trigger mechanoluminescence in a PDMS film to evaluate the potential of sonication-driven polymer mechanochemistry for such applications. Bis(adamantyl)-1,2-dioxetanes that are functionalized with polymers at both adamantane groups are known to cleave under mechanical force while exhibiting thermal stability up to 150 °C (8, 42). Upon scission of the dioxetane, a weakly luminescent excited-state ketone is formed. In the presence of fluorescent acceptor molecules such as 9,10-diphenylanthracene (DPA), more efficient chemiluminescence is observed (Fig. 1C). Using the data acquired from HIFU experiments on NP-containing PDMS films as references for transducer and pressure settings, we sonicated 5.0-mm-thick PDMS samples containing 1.5 wt % of covalently incorporated 1,2-dioxetane mechanophore and 0.5 wt % of noncovalently dispersed DPA. When the dioxetane-functionalized PDMS was irradiated with a 550-kHz HIFU transducer at the pressure level of 3.2 MPa (I_{SPTA} = 333 W·cm^{-2}) for 7 s, we observed a distinguishable blue luminescence [wavelength of ∼420 nm (38)] within the focal spot (Fig. 5). Once HIFU transduction stopped, the luminescence diminished immediately. The HIFU activation of mechanoluminescence was recorded with a digital camera and individual frames analyzed to quantify the intensity of luminescence (Fig. 5A and Movie S5). The optical images obtained show the emission, increase, and dilution of the intensity of blue luminescence with increasing time (Fig. 5B). This observation is consistent with the optomechanical tests reported in the literature (8), demonstrating that mechanical scission of the 1,2-dioxetane ring results in luminescence in the presence of DPA as an excited-state acceptor. We found that the diameter of the focal spot where the blue luminescence was recorded was almost identical to the beamwidth

Fig. 4. Sonication of the hemisphere NP-PDMS through mouse skull tissue (maximum length of 1 cm) with 3.2 MPa: (A) Image of the hemispherical NP-PDMS and prepared skull; (B) attenuated intensity in the time-domain signal due to the existence of the skull from hydrophone measurements; (C) skull–NP-PDMS assembly without sonication; (D) colored (orange) area by through-skull sonication (approximate diameter of 1.4 mm); and (E) disappearance of color after sonication. (Scale bar: 2.5 mm.)

Fig. 5. Mechanoluminescent behavior of dioxetane-functionalized PDMS: (*A*) Plot of the generated blue-light intensity versus time (a.u., arbitrary units); and (*B*) optical images showing the intensity versus HIFU irradiation time. The intensity plot is based on light generated in the focal spot (∼2.25 mm, 550 kHz). Green- and red-colored points in the plot indicate the start and end points of sonication, respectively. (Scale bar: 5.0 mm.)

(∼2.2 mm). A control experiment using a PDMS film containing 1.5 wt % 1,2-dioxetane and 0.5 wt % DPA (both noncovalently dispersed in the polymer matrix) did not generate blue light upon HIFU excitation (Fig. 1*D*). This demonstrates that the 1,2-dioxetane mechanophore must be covalently incorporated into the elastomer to elicit photoluminescence upon HIFU irradiation. The same set of ultrasound parameters (frequency and intensity) actuates both the mechanoluminescence of 1,2-dioxetane and the mechanochromism of NP with similar spatiotemporal precision. In contrast to mechanochromic activation of NP that occurs through an electrocyclic isomerization that is reversible via the absorption of energy from visible light, mechanical activation of the 1,2-dioxetane mechanophore results in irreversible cycloelimination. We found that when using HIFU to irradiate the same focal spot on a 1,2-dioxetane–functionalized PDMS film, only a few repetitions of light emission were possible, which is consistent with the irreversible consumption of mechanophores upon mechanical cleavage of the 1,2-dioxetane ring. Overall, we demonstrated that HIFU

activates mechanoluminesence in a PDMS polymer matrix, allowing control of light generation through a remote, noninvasive stimulus. By exploiting current advances in mechanophore-based chemoluminescence (43), the coupling of polymer mechanochemistry with HIFU techniques will facilitate the development of functional optogenetic tools (44).

Conclusion

This work demonstrates that HIFU is an efficient stimulus for noninvasive activation of polymer mechanochemistry in elastomeric PDMS networks. The advantage of the proposed method over existing triggering methods is the capability to achieve spatiotemporal control of mechanophore activation. In particular, while previous studies have demonstrated mechanochemical activation in bulk polymers using compression and tension (3, 4, 8, 45), the HIFU-based triggering system demonstrated here is a remote energy source capable of localizing the region of activation and triggering polymer mechanochemistry noninvasively.

These advances enable mechanoactivation of two different mechanophore systems. Both the isomerization of NP and the cycloelimination of 1,2-dioxetane were achieved using mechanical energy delivered from HIFU irradiation, leading to color change or blue-light emission within the focal spot on functionalized PDMS films. Given the broad library of productive mechanophores reported in the literature, we envision that HIFU-based triggering systems will open a route for exploiting polymer mechanochemistry for biomedical applications. One application we are currently exploring is the use of mechanoluminescent polymer systems to generate a localized photon flux noninvasively. Integrated with existing optogenetic techniques (44, 46, 47), this potentially provides a therapeutic platform that leverages the advantages of the optogenetic technology.

Materials and Methods

Preparation of PDMS with NP or NP-Control. The chromogenic PDMS samples contain 1.5 wt % of the vinyl-terminated NP, covalently incorporated into the elastomeric network, and were prepared using a Sylgard 184 kit. In a typical procedure, NP (160 mg) was dissolved in 300 μL of xylenes in a 15-mL polypropylene conical tube. Sylgard 184 prepolymer base (9.57 g) was added and the mixture stirred briefly and then vigorously mixed by vortex. The Sylgard 184 curing agent (950 mg) was then added and vigorously mixed until a homogeneous off-white consistency was obtained. The mixture was poured onto a 50-mm-diameter Teflon-lined Petri dish, and air bubbles removed by placing under high vacuum for 2 h. The prepolymer was oven cured at 65 °C overnight to form transparent films that peeled cleanly from the mold. The hemisphere-shaped samples were cast in a 40-mm-diameter hollow ball (1-Star Table Tennis Ball; Stiga), which was peeled off after curing.

Preparation of PDMS with 1,2-Dioxetane or 1,2-Dioxetane Control. The mechanoluminescent PDMS samples contain 1.5 wt % of the vinyl-terminated 1,2-dioxetane and 0.5 wt % of DPA as a fluorescent energy harvester. The 1,2-dioxetane (30 mg) and DPA (10 mg) were dissolved in 200 μL of xylenes and passed through a 0.45-μm syringe filter into a 20-mL scintillation vial. Sylgard 184 prepolymer base (1.95 g) was added, and then the mixture was mixed vigorously. Some precipitation of DPA was observed. Sylgard 184 curing agent (195 mg) was then added and the vial vortexed until thoroughly incorporated. The mixture was poured into a 50-mm-diameter Teflon-coated Petri dish, placed under high vacuum for 2 h, then cured at 65 °C overnight.

Design of HIFU Setup. To evaluate chromogenic responses in PDMS films, a HIFU-based triggering system was designed (Fig. 2A and *SI Appendix, SI Materials and Methods*). Note that the acoustic properties of PDMS materials (e.g., speed of sound, attenuation coefficient, etc.) and beam characteristics were measured (48) and summarized in *SI Appendix, SI Materials and Methods*. We first considered the geometry of the sample–holder assembly (Fig. 2 A, a3) because force-driven activation is affected by the geometry of the setup. Two ring-shaped polycarbonate plates were employed to circumferentially hold the PDMS samples (Fig. 2 A, a3) and the circumferential

margin (<5 mm) of the sample was sandwiched between two rings while the center (>45 mm) was freely exposed to degassed water (21 ± 2 °C) in the longitudinal direction (x direction). There is no substrate in the longitudinal direction that causes the reflection of the pressure field. In this configuration, the size of the beamwidth becomes more than one order of magnitude smaller than that of the sample (with a ratio of 0.05), ensuring the stress development on the focal spot without significant geometric distortions. This enables better understanding of the relationship between HIFU-induced pressure and the mechanophore activation. With this boundary condition, the acoustic pressure applied at the focal spot was estimated. It is important to note that the estimation of the acoustic pressure is only possible for this boundary condition because for more complicated boundary conditions, e.g., tissue, the boundary-induced intervention should be taken into account for the pressure calibration.

Spatial control of HIFU irradiation was achieved using a computer-controlled micropositioning system, which allowed the positioning of the sample–holder assembly at the focal distance with better than 2-μm spatial accuracy. The assembly mounted onto the positioning system was precisely placed at the focal distance of the transducer with its face (y–z direction) perpendicular to the beam of the transducer. Thereafter, the focal spot was determined by adjusting the vertical location (z direction) of the sample assembly. To achieve temporal resolution, we varied the duration and exposure level of CW-HIFU exposure. The results confirmed that by using a short sonication duration of 7 s and lower exposure levels (acoustic pressure below 3.2 MPa), a transfer of primarily mechanical energy was successfully achieved while minimizing heat-induced bulk material damage that can occur from accumulation of CW-HIFU–induced thermal energy into the PDMS films.

To control acoustic pressure in the setup, input voltage set in the function generator to the HIFU transducer was first calibrated with the output voltage of the beam at the focal point as recorded by a calibrated hydrophone, and then the conversion of the peak-to-peak amplitude of the output voltage to the acoustic pressure was achieved with the hydrophone sensitivity (*SI Appendix*, Fig. S5A). With this input, the acoustic pressure (or power) of the ultrasound beam at the focus was estimated (*SI Appendix*, Fig. S5B), and thus the corresponding intensity, I_{SPTA} and the radiation force, F (49) were obtained (*SI Appendix, SI Materials and Methods*). Based on this, the HIFU-triggering system generates the targeted pressure at the focus during the operation.

HIFU Sonication Through Skull. Use of animal materials in our lab has been approved by the Institutional Animal Care and Use Committee at the University of Illinois at Urbana–Champaign, adhering to NIH and US Department of Agriculture guidelines.

1. Caruso MM, et al. (2009) Mechanically-induced chemical changes in polymeric materials. *Chem Rev* 109:5755–5798.
2. Li J, Nagamani C, Moore JS (2015) Polymer mechanochemistry: From destructive to productive. *Acc Chem Res* 48:2181–2190.
3. Davis DA, et al. (2009) Force-induced activation of covalent bonds in mechanoresponsive polymeric materials. *Nature* 459:68–72.
4. Robb MJ, et al. (2016) Regioisomer-specific mechanochromism of naphthopyran in polymeric materials. *J Am Chem Soc* 138:12328–12331.
5. Göstl R, Sijbesma RP (2016) π-extended anthracenes as sensitive probes for mechanical stress. *Chem Sci (Camb)* 7:370–375.
6. Robb MJ, Moore JS (2015) A retro-staudinger cycloaddition: Mechanochemical cycloelimination of a β-lactam mechanophore. *J Am Chem Soc* 137:10946–10949.
7. Jakobs RTM, Ma S, Sijbesma RP (2013) Mechanocatalytic polymerization and crosslinking in a polymeric matrix. *ACS Macro Lett* 2:613–616.
8. Chen Y, et al. (2012) Mechanically induced chemiluminescence from polymers incorporating a 1,2-dioxetane unit in the main chain. *Nat Chem* 4:559–562.
9. Larsen MB, Boydston AJ (2013) "Flex-activated" mechanophores: Using polymer mechanochemistry to direct bond bending activation. *J Am Chem Soc* 135:8189–8192.
10. Gossweiler GR, et al. (2014) Mechanochemical activation of covalent bonds in polymers with full and repeatable macroscopic shape recovery. *ACS Macro Lett* 3:216–219.
11. Larsen MB, Boydston AJ (2014) Successive mechanochemical activation and small molecule release in an elastomeric material. *J Am Chem Soc* 136:1276–1279.
12. Grady ME, Beiermann BA, Moore JS, Sottos NR (2014) Shockwave loading of mechanochemically active polymer coatings. *ACS Appl Mater Interfaces* 6:5350–5355.
13. Sung J, Robb MJ, White SR, Moore JS, Sottos NR (2018) Interfacial mechanophore activation using laser-induced stress waves. *J Am Chem Soc* 140:5000–5003.
14. Li J, et al. (2014) Mechanophore activation at heterointerfaces. *J Am Chem Soc* 136: 15925–15928.
15. May PA, Moore JS (2013) Polymer mechanochemistry: Techniques to generate molecular force via elongational flows. *Chem Soc Rev* 42:7497–7506.
16. Zhang Y, Yu J, Bomba HN, Zhu Y, Gu Z (2016) Mechanical force-triggered drug delivery. *Chem Rev* 116:12536–12563.
17. Wang J, Kaplan JA, Colson YL, Grinstaff MW (2017) Mechanoresponsive materials for drug delivery: Harnessing forces for controlled release. *Adv Drug Deliv Rev* 108:68–82.
18. Cai P, et al. (2018) Biomechano-interactive materials and interfaces. *Adv Mater* 30: e1800572.
19. Amjadi M, Sheykhansari S, Nelson BJ, Sitti M (2018) Recent advances in wearable transdermal delivery systems. *Adv Mater* 30:1704530.
20. Rother M, Nussbaumer MG, Renggli K, Bruns N (2016) Protein cages and synthetic polymers: A fruitful symbiosis for drug delivery applications, bionanotechnology and materials science. *Chem Soc Rev* 45:6213–6249.
21. Brantley JN, Bailey CB, Wiggins KM, Keatinge-Clay AT, Bielawski CW (2013) Mechanobiochemistry: Harnessing biomacromolecules for force-responsive materials. *Polym Chem* 4:3916–3928.

22. Jacobs MJ, Blank K (2014) Joining forces: Integrating the mechanical and optical single molecule toolkits. *Chem Sci* 5:1680–1697.
23. Kennedy JE (2005) High-intensity focused ultrasound in the treatment of solid tumours. *Nat Rev Cancer* 5:321–327.
24. Zhou Y-F (2011) High intensity focused ultrasound in clinical tumor ablation. *World J Clin Oncol* 2:8–27.
25. Brown MRD, Farquhar-Smith P, Williams JE, ter Haar G, deSouza NM (2015) The use of high-intensity focused ultrasound as a novel treatment for painful conditions-a description and narrative review of the literature. *Br J Anaesth* 115:520–530.
26. Quadri SA, et al. (2018) High-intensity focused ultrasound: Past, present, and future in neurosurgery. *Neurosurg Focus* 44:E16.
27. Leinenga G, Langton C, Nisbet R, Götz J (2016) Ultrasound treatment of neurological diseases–current and emerging applications. *Nat Rev Neurol* 12:161–174.
28. Xiong X, et al. (2015) Remote spatiotemporally controlled and biologically selective permeabilization of blood-brain barrier. *J Control Release* 217:113–120.
29. Hynynen K (2008) Ultrasound for drug and gene delivery to the brain. *Adv Drug Deliv Rev* 60:1209–1217.
30. Sirsi SR, Borden MA (2014) State-of-the-art materials for ultrasound-triggered drug delivery. *Adv Drug Deliv Rev* 72:3–14.
31. Liang X, et al. (2015) Nanohybrid liposomal cerasomes with good physiological stability and rapid temperature responsiveness for high intensity focused ultrasound triggered local chemotherapy of cancer. *ACS Nano* 9:1280–1293.
32. van Elk M, et al. (2014) Triggered release of doxorubicin from temperature-sensitive poly(N-(2-hydroxypropyl)-methacrylamide mono/dilactate) grafted liposomes. *Biomacromolecules* 15:1002–1009.
33. Dromi S, et al. (2007) Pulsed-high intensity focused ultrasound and low temperature-sensitive liposomes for enhanced targeted drug delivery and antitumor effect. *Clin Cancer Res* 13:2722–2727.
34. Tong R, Lu X, Xia H (2014) A facile mechanophore functionalization of an amphiphilic block copolymer towards remote ultrasound and redox dual stimulus responsiveness. *Chem Commun (Camb)* 50:3575–3578.
35. Kim G, et al. (2019) Data from "Molecular structure of bis-vinyl terminated NP." Cambridge Structural Database. Available at https://www.ccdc.cam.ac.uk/structures/Search?Ccdcid=1890871&DatabaseToSearch=Published. Deposited January 14, 2019.
36. Liu B, Xia H, Fei G, Li G, Fan W (2013) High-intensity focused ultrasound-induced thermal effect for solid polymer materials. *Macromol Chem Phys* 214:2519–2527.
37. Rudenko OV, Sarvazyan AP, Emelianov SY (1996) Acoustic radiation force and streaming induced by focused nonlinear ultrasound in a dissipative medium. *J Acoust Soc Am* 99:2791–2798.
38. Hui W, et al. (2015) Biocompatible PEG-chitosan@Carbon dots hybrid nanogels for two-photon fluorescence imaging, near-infrared light/pH dual-responsive drug carrier, and synergistic therapy. *Adv Funct Mater* 25:5537–5547.
39. Miller DL, et al.; Bioeffects Committee of the American Institute of Ultrasound in Medicine (2012) Overview of therapeutic ultrasound applications and safety considerations. *J Ultrasound Med* 31:623–634.
40. Hynynen K, et al. (2001) MR imaging-guided focused ultrasound surgery of fibroadenomas in the breast: A feasibility study. *Radiology* 219:176–185.
41. Nguyen TN, Do MN, Oelze ML (2019) Visualization of the intensity field of a focused ultrasound source *in situ*. *IEEE Trans Med Imaging* 38:124–133.
42. Clough JM, Creton C, Craig SL, Sijbesma RP (2016) Covalent bond scission in the Mullins effect of a filled elastomer: Real-time visualization with mechanoluminescence. *Adv Funct Mater* 26:9063–9074.
43. Yuan W, Yuan Y, Yang F, Wu M, Chen Y (2018) Improving mechanoluminescent sensitivity of 1,2-dioxetane-containing thermoplastic polyurethanes by controlling energy transfer across polymer chains. *Macromolecules* 51:9019–9025.
44. Raman R, et al. (2016) Optogenetic skeletal muscle-powered adaptive biological machines. *Proc Natl Acad Sci USA* 113:3497–3502.
45. Kosuge T, Imato K, Goseki R, Otsuka H (2016) Polymer–inorganic composites with dynamic covalent mechanochromophore. *Macromolecules* 49:5903–5911.
46. Deisseroth K (2011) Optogenetics. *Nat Methods* 8:26–29.
47. Yizhar O, Fenno LE, Davidson TJ, Mogri M, Deisseroth K (2011) Optogenetics in neural systems. *Neuron* 71:9–34.
48. Kemmerer JP, Oelze ML (2012) Ultrasonic assessment of thermal therapy in rat liver. *Ultrasound Med Biol* 38:2130–2137.
49. Nightingale K, Soo MS, Nightingale R, Trahey G (2002) Acoustic radiation force impulse imaging: In vivo demonstration of clinical feasibility. *Ultrasound Med Biol* 28:227–235.

Kim et al.